



Retrieval of aerosol absorption properties

E. Rodríguez et al.

Retrieval of aerosol absorption properties using the AATSR satellite instrument: a case study of wildfires over Russia 2010

E. Rodríguez¹, P. Kolmonen¹, T. H. Virtanen¹, L. Sogacheva¹, A.-M. Sundström², and G. de Leeuw^{1,2}

¹Climate Change Unit, Finnish Meteorological Institute, Erik Palmén Aukio 1, 00101, Helsinki, Finland

²Dept. of Physics, Helsinki, University of Helsinki, Helsinki, Finland

Received: 20 August 2014 – Accepted: 6 September 2014 – Published: 23 September 2014

Correspondence to: E. Rodríguez (edith.rodriguez@fmi.fi)

Published by Copernicus Publications on behalf of the European Geosciences Union.

Title Page

Abstract

Introduction

Conclusions

References

Tables

Figures



Back

Close

Full Screen / Esc

Printer-friendly Version

Interactive Discussion



Abstract

The retrieval of aerosol properties from satellite data is based on the optimized fit of simulated and measured radiances at the top of the atmosphere (TOA). The simulations are made using a radiative transfer model with a variety of representative aerosol properties. The optimum fit is obtained for a certain combination of aerosol components, which are externally mixed to provide the aerosol model which in turn is used to calculate the aerosol optical depth (AOD). However, other aerosol properties could be provided. In the aerosol retrieval algorithm (ADV) applied to data from the Advanced Along Track Scanning Radiometer (AATSR), four aerosol components are used, each of which is defined by their (lognormal) size distribution and a complex refractive index. The fine mode fraction is a continuous mixture of weakly and strongly absorbing components which allows for the definition of any absorbing aerosol model within the specified limits. Hence, assuming that the correct aerosol model is selected during the retrieval process, also the single scattering albedo (SSA) should correctly be retrieved. In this paper we present the SSA retrieval using the ADV algorithm by application to wildfires over Russia in the summer of 2010. Together with the AOD, the SSA provides the aerosol absorbing optical depth (AAOD). The results are compared with AERONET data, i.e. AOD level 2.0 and SSA and AAOD inversion products. The RMSE is 0.03 for SSA and 0.02 for AAOD. The SSA is further evaluated by comparison with the SSA retrieved from the Ozone Monitoring Instrument (OMI). The SSA retrieved from both instruments show similar features, but the AATSR-retrieved SSA values over areas affected by wildfires are lower.

1 Introduction

Aerosol particles have a significant effect on Earth's climate by perturbing the radiation balance both directly, due to scattering and absorption of solar radiation, and indirectly, due to their effect on cloud micro physical properties (IPCC, 2007). Aerosols are also

AMTD

7, 9839–9868, 2014

Retrieval of aerosol absorption properties

E. Rodríguez et al.

Title Page

Abstract

Introduction

Conclusions

References

Tables

Figures



Back

Close

Full Screen / Esc

Printer-friendly Version

Interactive Discussion



Retrieval of aerosol absorption properties

E. Rodríguez et al.

Title Page

Abstract

Introduction

Conclusions

References

Tables

Figures



Back

Close

Full Screen / Esc

Printer-friendly Version

Interactive Discussion



important because of their effects on health and air quality. Aerosol particles originate from human activity and natural sources, by direct generation or by secondary formation from their precursor gases. Effects due to particles generated by human activity (anthropogenic aerosols) need to be considered in the context of effects from particles of natural origin. The assessment of aerosol effects on climate requires information on both the aerosol amount and on other characteristics, such as size, composition and optical properties including absorption (Russell et al., 2010) which is the focus of this paper. Many studies have been conducted on the absorption of aerosols using model simulations, ground-based in situ measurements and different remote sensing techniques utilizing ground based measurements and satellite retrievals (Goto et al., 2011; Satheesh et al., 2009; Medina et al., 2012; Liu et al., 2011). A measure for the aerosol absorption is the single scattering albedo (SSA), defined as the ratio of aerosol scattering to aerosol extinction (the sum of scattering and absorption) which for satellite observations relates to the column properties, i.e. scattering optical depth to the total optical depth (scattering + absorption) of the atmosphere. It is a dimensionless quantity with values between 0 and 1.

Satellites provide information on the spatial distribution of aerosols on regional to global scales. Several satellite remote sensing studies have been reported on the retrieval of aerosol absorption properties, represented typically by the SSA. Kahn et al. (2010) presented the latest version (V22) of the MISR algorithm including SSA retrieval, which helps to distinguish between different airmasses. Patadia et al. (2013) presented MISR research retrieval results to evaluate the performance of the MISR V22 Standard aerosol retrieval algorithm. Torres et al. (2013) introduced the combined use of OMI, CALIOP and AIRS observations for the characterization of aerosol properties as an improvement over OMI aerosol retrieval capabilities. Jethva and Torres (2011) showed the improvement in the OMAERUV algorithm by evaluating the OMAERUV products of AOD and SSA against the AERONET measurements over the biomass burning regions of South America, central Africa, and northern India. In Zhu et al. (2011) a method to

retrieve the SSA during polluted days, using a critical reflectance technique, is applied to MODIS data obtained over biomass to burning regions.

In this paper the Advanced Along Track Scanning Radiometer (AATSR) dual view (ADV) aerosol retrieval algorithm is used to provide an estimate of the SSA. The primary parameter retrieved from AATSR data is the aerosol optical depth (AOD) for cloud-free scenarios. The AOD is obtained by minimizing the difference between the computed and measured reflectances at the top of the atmosphere (TOA), simultaneously at three wavelengths, using a least squares method. In this procedure the TOA reflectance is computed using a radiative transfer model in which the mixing ratio of different aerosol components, described below, is continuously varied. The mixing ratio providing the minimum difference between the computed and observed TOA reflectance is used to compute the AOD (de Leeuw et al., 2014; Veeffkind et al., 1999; Curier et al., 2009; Kolmonen et al., 2013). However, because the aerosol properties provide the basis for the computation, they could also be used to provide other aerosol properties such as the SSA. In this paper we evaluate how well the SSA retrieval works based on a study of the retrieval of AOD and SSA, using AATSR data, over wildfires over western Russia in the summer of 2010. The SSA and AAOD (AAOD = AOD(1-SSA)) are compared against data obtained from the AERONET level 2.0 inversion product (Dubovik et al., 1998, 2000, 2002), and further evaluated by comparison with the SSA retrieved from the Ozone Monitoring Instrument (OMI).

2 SSA retrieval methods

2.1 Retrieval of the single scattering albedo for fine particles using the AATSR Dual View (ADV) algorithm

The AATSR instrument provides two views of the earth surface, one near-nadir and one at a forward angle of 55° . For each of these views, the radiances are measured at 7 wavelengths from the visible to the thermal infrared. Aerosol properties are retrieved

Retrieval of aerosol absorption properties

E. Rodríguez et al.

Title Page

Abstract

Introduction

Conclusions

References

Tables

Figures



Back

Close

Full Screen / Esc

Printer-friendly Version

Interactive Discussion



Retrieval of aerosol absorption properties

E. Rodríguez et al.

[Title Page](#)[Abstract](#)[Introduction](#)[Conclusions](#)[References](#)[Tables](#)[Figures](#)[Back](#)[Close](#)[Full Screen / Esc](#)[Printer-friendly Version](#)[Interactive Discussion](#)

at the four shortest wavelengths (0.555, 0.659, 0.865 and 1.61 μm) and some of these, together with the longer ones, are used for cloud screening. Over land the surface reflectance, which often overwhelms the aerosol signal at TOA, is accounted for by using both views. The dual view (ADV) algorithm used in this study has been developed for retrieval of aerosol optical properties over land (Veefkind et al., 1999, 2000; Robles Gonzáles, 2003; Curier et al., 2009; Kolmonen et al., 2013). These properties include the aerosol optical depth (AOD) at three wavelengths (nominally 0.555, 0.659 and 1.61 μm) and the Ångström exponent, but also the mixing ratio of the aerosol components (see below) is available.

In the ADV algorithm, the reflectances measured in the nadir and forward views are used together to eliminate surface reflectance effects and thus retain only the path reflectance. The path reflectance is used to determine AOD for the best fitting combination of aerosol components, as indicated in the introduction. As described in de Leeuw et al. (2014), the four aerosol components used are described by a lognormal size distribution defined by an effective radius and standard deviation, and a complex refractive index (see Table 1).

Two of the aerosol components describe fine mode aerosol particles, assumed to be spherical, and the other two describe the properties of coarse mode aerosol particles. One of the fine mode components is weakly absorbing and the other one is strongly absorbing. By mixing these two components the absorbing properties of the fine mode particles can be continuously varied between these two extremes. The coarse mode aerosol particle components represent sea salt aerosol (spherical) and desert dust aerosol (non-spherical). The final aerosol model is determined by first mixing each of the fine and coarse components separately, and finally mixing the ensuing fine and coarse components into a bi-modal lognormal size distribution with associated optical properties.

The TOA reflectances are computed using a radiative transfer method (de Haan et al., 1987) for individual aerosol components. However, these computations are very time-consuming and there look-up tables (LUTs) are created for certain discrete

sun-satellite geometries and aerosol loads. During the retrieval the weight of each component is varied:

$$\tau(\lambda) = b_1[b_2\tau_{\text{wa}}(\lambda, L) + (1 - b_2)\tau_{\text{sa}}(\lambda, L)] + (1 - b_1)[b_{\text{dust}}\tau_{\text{dust}}(\lambda, L) + (1 - b_{\text{dust}})\tau_{\text{ss}}(\lambda, L)], \quad (1)$$

where b_1 is the fraction of fine particles, b_2 is the fraction of non-absorbing fine particles, and b_{dust} is the dust fraction. AOD is a function of wavelength λ . The retrieved parameters are the two mixtures (b_1 , b_2), and L is the measure of the aerosol loading. The measure L is used to determine aerosol properties, such as AOD, reflectance, and transmittance due to aerosols, from the LUTs. Generally, the higher L , the higher the aerosol loading. The dust fraction is not retrieved but is provided from a climatology derived as the median of 13 AEROCOM models (cf. de Leeuw et al., 2014). The abbreviations are: wa – weakly absorbing fine component, sa – strongly absorbing fine component, and ss – sea salt coarse component.

During the retrieval, the atmospheric reflectance due to aerosol particles is calculated as indicated above. It is compared to the path reflectance determined from the radiance measured for cloud-free pixels by the AATSR instrument at TOA corrected for surface effects and molecular scattering. The linear mixing of reflectances from LUTs, however, does not correctly take into account the difference of absorbing properties between the aerosol components as shown by Abdou et al. (1997). Instead, a modified linear mixing is used. Adopted for the retrieval algorithm for two arbitrary aerosol components α and β the modified linear mixing of reflectance ρ is given by:

$$\rho_{\text{aer}} = b_\alpha \frac{\omega_{\text{mix}}}{\omega_\alpha} e^{-\tau_\alpha|\omega_\alpha - \omega_{\text{mix}}|} \rho_\alpha + b_\beta \frac{\omega_{\text{mix}}}{\omega_\beta} e^{-\tau_\beta|\omega_\beta - \omega_{\text{mix}}|} \rho_\beta, \quad (2)$$

Where ω is the single scattering albedo (SSA) and τ is the AOD. Subscript mix refers to the linear mixture of the two aerosol components. In practice $b_\beta = (1 - b_\alpha)$. Values for ω , τ and ρ come from the corresponding LUTs. It can be seen in Eq. (2) that the

Retrieval of aerosol absorption properties

E. Rodríguez et al.

Title Page

Abstract

Introduction

Conclusions

References

Tables

Figures



Back

Close

Full Screen / Esc

Printer-friendly Version

Interactive Discussion



absorption of an aerosol component affects the resulting reflectance ρ_{aer} through the SSA (ω). The dependence of the various terms in Eq. (2) on the wavelength and L are excluded from the equation for brevity.

In Table 1 refractive indices for the fine mode particles are listed for the wavelength of 0.555 μm . This value is also applied for the other wavelengths used in this study. However, although the particle size distributions for both fine mode components are identical, the SSA varies with wavelength because of the variation in the particle size parameters ($2\pi r/\lambda$) with wavelength, which determines the aerosol scattering and absorption, as shown in Table 2 for the two fine particle aerosol components at the AATSR wavelengths.

The different spectral behavior of the SSA of the two fine mode components leads to differences in their TOA reflectance spectra, as illustrated in Fig. 1 where the TOA reflectance for each of the aerosol components is plotted as a function of AOD, for each of the four AATSR wavelengths used in this study. The higher absorption of the strongly absorbing fine component results in lower reflectance values when compared to the weakly absorbing component reflectance. The phenomenon is wavelength dependent and increases with AOD. This, together with the modified linear reflectance mixture in Eq. (2), is the basis of the described SSA retrieval.

In the retrieval, the mixture b_2 (and also the fine mode fraction b_1 and the aerosol loading measure L) is sought that minimizes the difference, in a least square sense, between the measured and modelled aerosol reflectances. In practice, surface and Rayleigh reflectance are also taken into account and treated in the retrieval algorithm. The aerosol parameters (e.g., AOD, SSA) are subsequently determined from the aerosol model, i.e. a mixture of the components as determined by b_1 and b_2 , and the value of L . The resulting fine mode SSA ω is given by the linear mixture

$$\omega(\lambda) = b_2\omega_{\text{wa}}(\lambda) + (1 - b_2)\omega_{\text{sa}}(\lambda) \quad (3)$$

Table 2 gives the maximum and minimum values of the SSA that can be retrieved. While the retrieved AOD results from the mixture of all four aerosol components, in

Retrieval of aerosol absorption properties

E. Rodríguez et al.

Title Page

Abstract

Introduction

Conclusions

References

Tables

Figures

◀

▶

◀

▶

Back

Close

Full Screen / Esc

Printer-friendly Version

Interactive Discussion



Retrieval of aerosol absorption properties

E. Rodríguez et al.

Title Page

Abstract

Introduction

Conclusions

References

Tables

Figures



Back

Close

Full Screen / Esc

Printer-friendly Version

Interactive Discussion



5 this study we provide the retrieved SSA for the fine mode particles because our main interest is in testing the possible to retrieve SSA by application to biomass burning aerosol generated by forest fires, which mainly consist of fine mode aerosol particles. Furthermore, the difference in coarse particle reflectance, a mixture of sea salt and dust aerosol particles, is not large at the retrieval wavelengths except for high AOD. This is illustrated in Fig. 2 where the TOA reflectance for sea salt and dust aerosol components are plotted as function of AOD, for all four wavelengths considered in this study.

10 One limiting factor of the SSA retrieval is the aerosol concentration. While the modelled aerosol reflectances differentiate effectively at high AOD values, at low AOD levels the reflectance spectra for non-absorbing and absorbing aerosols are almost identical (Fig. 1). Thus, the AATSR measurement error may shadow the aerosol SSA influence. For this reason the SSA retrieval is limited to cases where the retrieved AOD at 0.555 μm has values larger than 0.2. To retrieve the SSA for coarse particles a very high AOD value would be needed to separate the TOA reflectance spectra of the two coarse components properly (Fig. 2). This could, however, be utilized in the detection and retrieval of large dust outbreaks.

2.2 OMI aerosol retrieval

20 OMI retrieval products are used in this work for comparison with the AATSR SSA results. The OMAERUV aerosol algorithm has been designed to produce the optical thickness and single scattering albedo of tropospheric aerosols over ocean and land. OMAERUV considers three major aerosol types: desert dust, carbonaceous aerosols associated with biomass burning, and weakly absorbing sulfate-based aerosols. Each aerosol type is represented by seven aerosol models with varying single scattering albedo, for a total of twenty-one micro-physical models. The extinction optical depth and single scattering albedo are retrieved by examining the variability of the relationship between radiances measured at 0.354 and 0.388 μm (Torres et al., 2002a, b, 25 2007).

2.3 AERONET inversion product

To validate the AOD and compared the AOD and SSA retrieved from AATSR using ADV as described above, AERONET (Holben et al., 1998) sun photometer measurements are used. AERONET provides the optical properties of aerosols at four wavelengths (440, 670, 870 and 1020 nm) as a retrieval product from the sun photometer sky radiance measurements (almucantar and principal plane) using an inverse code developed by Dubovik and co-authors (Dubovik and King, 2000; Dubovik et al., 2000). The current model version (Dubovik et al., 2006) accounts for particle non-sphericity with a spheroid model and retrieves the portion of non-spherical particles of the aerosol size distribution. The absolute error given by AERONET for the SSA is 0.03 and for the AOD 0.01. The optical properties such as the SSA are constrained for quality-assurance (level 2.0). This means that the SSA is retrieved only if AOD at 400 nm has a value greater than 0.4 and the solar zenith angle is larger than 50°.

3 Russian wildfires in the summer of 2010

During the summer of 2010, between the end of July and 18 August, hundreds of wildfires broke out across central Russia, primarily in the Southeastern part and extending to the vicinity of Moscow. Witte et al. (2011); Huijnen et al. (2012); Chubarova et al. (2012) and Mei et al. (2011), among others, give an overview of the weather conditions during this period. In summary, anti-cyclonic conditions persisted around Moscow during the first ten days of August. Heat waves persisted until 14 August, and the relative humidity levels over Moscow were very low with values of 20–40% (on average in August the humidity is around 77%, <http://meteoweb.ru/cl006-7.php>). The fires decreased from 13 August when the first rain arrived, and on 19 August the air cleaned up when the wind turned to the West, which is the most probable wind direction over Moscow.

During this period, the PM₁₀, CO, and NO_x concentrations exceeded almost continuously their maximum permissible concentrations (MPCs) during about 30 days

AMTD

7, 9839–9868, 2014

Retrieval of aerosol absorption properties

E. Rodríguez et al.

Title Page

Abstract

Introduction

Conclusions

References

Tables

Figures



Back

Close

Full Screen / Esc

Printer-friendly Version

Interactive Discussion



(Zvyagintsev et al., 2011). The highest concentrations were observed from 4 to 9 August. The unprecedented intensive heat wave provoked effects over distant areas like Kuopio in Eastern Finland (Mielonen et al., 2012). In view of the high biomass burning aerosol concentrations and expected high SSA values, we selected this period to evaluate the retrieval of SSA using AATSR data and the ADV algorithm. We focus on the August period when the largest AOD values were observed (Mei et al., 2011; Witte et al., 2011; Konovalov et al., 2011; Mielonen et al., 2012). Figure 3 shows the locations of the wildfires over Russia in August 2010.

4 Results

The spatial distributions of the AOD at 555 μm and SSA are shown for three periods in August 2010 in Fig. 4a–c. Each map shows values aggregated over the period indicated at the top of each figure. The AOD distributions are combined with 5 days back trajectories at 500 m (in purple) and 100 m (in grey). Figure 4a shows 5 day back trajectories arriving at Moscow on 11 August. The airmass at 500 m indicates transport of the forest fire plume during these 5 days to Moscow, where the AOD values were up to 2. On the other hand, the air mass arriving at 100 m indicates that at this level the air was not influenced by the forest fires and hence the atmospheric column was likely stratified with lower aerosol concentrations near the ground than higher up. However, we have no observational data, such as, e.g., lidar measurements, to confirm this.

The airmass arriving at Moscow on 12 August at the two altitudes indicate that cleaner air was transported from the west bringing rain (not shown here). Later, the airmass arriving in Moscow on 18 August shows how the air was transported again from the southeast with a high concentration of forest fire aerosol resulting in AOD values of up to 2. On 19 August the airmass originated again from the west and AOD values returned to normal values until the end of the month.

The aggregated SSA over the same area and for the same three periods in August 2010 is shown in Fig. 4d–f. The low SSA values in Fig. 4d and e indicate high

Retrieval of aerosol absorption properties

E. Rodríguez et al.

Title Page

Abstract

Introduction

Conclusions

References

Tables

Figures



Back

Close

Full Screen / Esc

Printer-friendly Version

Interactive Discussion



concentrations of absorbing particles. The areas with smaller SSA values coincide with areas with high AOD (Fig. 4a and b), i.e. it is likely that the smoke produced by the wild fires is the reason for the low SSA results. The decrease of the effect of forest fire aerosol, resulting in SSA values higher than 0.95, is evident after 19 August (Fig. 4f).

4.1 Comparison of AATSR retrieval and AERONET

The AOD and SSA retrieved from AATSR were compared with AERONET level 2.0 products. In this comparison, an area around each AERONET station of $1^\circ \times 1^\circ$ was used and the AERONET data were averaged over a time window of ± 10 h around the satellite overpass. This large time window was used to collect as many coincidences between the AATSR and AERONET SSAs as possible. The time difference may contribute to the scatter in the results, especially as the local dynamic changes in smoke plume conditions can be large in a very small time period.

Scatter plots of AOD and SSA retrieved from AATSR versus AERONET products are shown in Fig. 5. For the AOD, both data sets are in excellent agreement with a correlation coefficient (R) of 0.90, and a small negative bias of -0.09 . However, Fig. 5a shows that there are some outliers with AATSR-retrieved AOD values which are substantially higher than AERONET, for AOD 0.7. The mean AOD for this period is similar, 0.25 for AERONET and 0.24 for AATSR (Fig. 5a).

The SSA retrievals from AATSR are compared with the SSA inversion product from AERONET in Fig. 5b. As the AATSR SSA is retrieved at 555 nm, the AERONET values are determined by using linear interpolation between the SSA at 440 and 675 nm. The dotted lines in Fig. 5b indicate the ± 0.03 range uncertainty given by AERONET for the SSA inversion. The range of SSA variability for AATSR (0.81–0.97) is slightly different from that for AERONET (0.83–0.98).

A more detailed study on the discrepancy between the AATSR and AERONET SSA values was made using a root mean square error (RMSE) analysis. This parameter measures the difference between the values predicted by a model and the values actually observed from the environment that is being modelled. Here we can divide the

Retrieval of aerosol absorption properties

E. Rodríguez et al.

Title Page

Abstract

Introduction

Conclusions

References

Tables

Figures



Back

Close

Full Screen / Esc

Printer-friendly Version

Interactive Discussion



Retrieval of aerosol absorption properties

E. Rodríguez et al.

Title Page

Abstract

Introduction

Conclusions

References

Tables

Figures



Back

Close

Full Screen / Esc

Printer-friendly Version

Interactive Discussion



SSA retrievals in three cases; the first case includes the total days with SSA coincidences between AATSR and AERONET. Here the RMSE between the measurements is 0.05. The second case contains the SSA values retrieved with AATSR which are lower than 0.90, which includes 20% of the days where both instruments have results. For this case the RMSE is 0.08. The last case includes AATSR SSA values larger than 0.90, which has the largest amount of coincidences (80%) and an RMSE of 0.03. The results show a disagreement between the SSA results when the AATSR SSA is low, but in general we see a reasonable agreement between the retrieved SSA from AATSR and AERONET.

Figure 6 shows the spectral dependence of the AERONET-retrieved SSA on 7 August 2010. The SSA at 555 μm is around 0.95, indicating weakly absorbing particles. On the other hand, the SSA increases with wavelength in contrast to the expected behavior for fine mode particles (Fig. 1) but in line with a large influence of coarse particles for which the absorption increases with wavelength (Fig. 2). This may provide an explanation for the discrepancy between the SSA retrieved from AATSR and AERONET, since for the AATSR retrieval we only consider the effect of fine particles.

4.2 Evaluation of AATSR-retrieved SSA by comparison with OMI

For evaluation of the AATSR-retrieved SSA product, it is compared with OMI SSA. Here we use a $1^\circ \times 1^\circ$ pixel area, with daily resolution. We consider only pixels for which data from both satellites are available. The difference plot, i.e. OMI-AATSR SSA in Fig. 7 shows that there are both positive and negative values, but overall the OMI SSA is higher than that of AATSR. On average the SSA difference over the study area is 0.1. As with the AERONET comparison, AATSR seems to indicate that absorbing aerosol occurs over the whole study area affected by wild fires, whereas OMI often provides higher SSA values, i.e. the occurrence of less absorbing aerosol. It is noted that the maximum SSA value at 0.555 μm which can be retrieved with AATSR is 0.977, for weakly absorbing aerosol (see Table 1) (de Leeuw et al., 2014). This difference may in part explain some of the differences between AATSR and OMI. It is also important

Retrieval of aerosol absorption properties

E. Rodríguez et al.

Title Page

Abstract

Introduction

Conclusions

References

Tables

Figures

◀

▶

◀

▶

Back

Close

Full Screen / Esc

Printer-friendly Version

Interactive Discussion



to note that there is a difference of three hours between the satellite overpasses due to the diurnal variations in the emissions, which could affect the atmospheric conditions between the two measurements (Krol et al., 2013). The total RMSE value between the retrievals is 0.05. Looking in more detail, similar to the RMSE analysis for comparison with AERONET SSA, we observe that for AATSR SSA lower than 0.90 (16% of the cases), the RMSE is 0.11. However, for AATSR-retrieved SSA larger than 0.95 (25% of the cases) the RMSE is 0.03, i.e. good agreement. The remaining 59% are cases with AATSR SSA values between 0.90 and 0.95. For these cases the RMSE is 0.04. Even though the results show that there is some disagreement between both satellites retrievals as regards how much the aerosol actually absorb, they do agree over areas where the forest fires are.

As an extension of the case study, we present the global SSA retrieved from AATSR for the month September 2010. In Fig. 8 (bottom panel) we show the locations of wild fires in September 2010. A good correspondence is observed between the wild fire locations and the low SSA values in Fig. 8 (top panel).

4.3 AOD Retrievals

The absorbing properties of the aerosols are often expressed in terms of the absorbing aerosol optical depth (AAOD), which is defined as: $AAOD = AOD(1 - SSA)$. Figure 9 shows a scatterplot of the AAOD obtained with AATSR versus the AERONET inversion product. The results are similar for low AAOD (< 0.05) but there are some outliers with very high AAOD values retrieved from AATSR. The green lines in Fig. 9 are the estimated uncertainty of the AAOD given for AERONET (0.01). The RMSE between the retrievals is 0.06. When we analyze the cases where the AAOD is lower than 0.05 (74% of the cases) the RMSE is 0.02 and when the AAOD is larger than 0.05 (26% of the cases) the RMSE is 0.11. Similar to SSA retrieval, also the AAOD comparison with AERONET data shows underestimation of AATSR retrieved AAOD as compared with the AERONET values.

5 Conclusions

A method to retrieve the SSA with the AATSR satellite instrument has been presented. The AOD and SSA retrievals allow us to estimate the effect of the wildfires over Russia in 2010 on these parameters. The smoke-affected area can be clearly observed both in the AOD and SSA patterns. AOD increased up to 2 during the wild fire period. The SSA values show generally reasonable agreement with both retrieval methods used for comparison, AERONET and OMI, but there are cases for which large discrepancies are observed and hence the method needs further development before it can provide quantitative results. The general results show an RMSE of 0.05 when compared with both AERONET and OMI.

Future improvement is needed in the quantitative estimation of absorbing aerosol properties from satellite data. AATSR can distinguish the area affected by wild fires but cannot give accurate quantitative information about how absorb the aerosol particles actually are. The RMSE decreases to 0.03 in the comparison with AERONET when the low SSA retrievals from AATSR are discarded. In the case of OMI, when the low values are not taken into consideration the RMSE decreases to 0.04. We consider that for both comparisons the agreement is reasonable, taking into account the differences between the retrieval techniques and the temporal and spatial issues in each comparison.

The AAOD retrievals confirm the SSA results, and also point out the good behaviour between the AOD retrievals. The RMSE is 0.02 when the AAOD is low, which represents the 74% of the cases. It is noted that AAOD is derived from SSA and AOD and the two quantities are thus not independent.

The global SSA map shows a clear connection between the occurrence of forest fires over Africa and the Amazons and the areas where the SSA is expected to have low values. The retrievals presented here provide a tool for a qualitative indication of the forest fires location, and especially resulting smoke plume coverage.

Acknowledgements. The study presented in this manuscript contributes to the objectives of the Centre on Excellence in Atmospheric Science funded by the Finnish Academy of Sciences

Retrieval of aerosol absorption properties

E. Rodríguez et al.

Title Page

Abstract

Introduction

Conclusions

References

Tables

Figures



Back

Close

Full Screen / Esc

Printer-friendly Version

Interactive Discussion



Excellence (project no. 272041), the projects Aerosol-cci (ESA-ESRIN project AO/1-6207/09/I-LG), Globemission (ESA-ESRIN Data Users Element (DUE), project AO/1-6721/11/I-NB), PE-GASOS (EU FP7 ENV.2010.1.1.2-1) and MEGAPOLI (EU FP7 FP7-ENV-2007.1.1.2.1).

References

- 5 Abdou, W. A., Martonchik, J. V., Kahn, R. A., West, R. A., and Diner, D. J.: A modified linear-mixing method for calculating atmospheric path radiances of aerosol mixtures, *J. Geophys. Res.*, 102, D14,16883-16888, 1997. 9844
- Chubarova, N., Nezval', Ye., Sviridenkov, I., Smirnov, A., and Slutsker, I.: Smoke aerosol and its radiative effects during extreme fire event over Central Russia in summer 2010, *Atmos. Meas. Tech.*, 5, 557–568, doi:10.5194/amt-5-557-2012, 2012. 9847
- 10 Curier, R. L., de Leeuw, G., Kolmonen, P., Sundström, A-M., Sogacheva, L., and Benouna, Y. S.: Satellite Aerosol Remote Sensing Over Land, edited by: Kokhanovsky, A. A. and de Leeuw, G., Springer-Praxis, UK, 135–160, 2009. 9842, 9843
- de Haan, J. F., Bosma, B. P., and Howenier, J. W.: The adding method for multiple scattering calculations of polarized light, *Astron. Astrophys.*, 183, 371–391, 1987. 9843
- 15 de Leeuw, G., Holzer-Popp, T., Bevan, S., Davies, W., Descloîtres, J., Grainger, R. G., Griesfeller, J., Heckel, A., Kinne, S., Klüser, L., Kolmonen, P., Litvinov, P., Martynenko, D., North, P. J. R., Ovigneur, B., Pascal, N., Poulsen, C., Ramon, D., Schulz, M., Siddans, R., Sogacheva, L., Tanré, D., Thomas, G. E., Virtanen, T. H., von Hoyningen-Huene, W., Vountas, M., and Pinnock, S.: Evaluation of seven European aerosol optical depth retrieval algorithms for climate analysis, *Remote Sens. Environ.*, in press, 2014. 9842, 9843, 9844, 9850, 9858
- Dubovik, O. and King, M. D.: A flexible inversion algorithm for retrieval of aerosol optical properties from Sun and sky radiance measurements, *J. Geophys. Res.*, 105, 20673–20696, 2000. 9847
- 25 Dubovik, O., Holben, B. N., Kaufman, Y. J., Yamasoe, M., Smirnov, A., Tanrò, D., and Slutsker, I.: Single-scattering albedo of smoke retrieved from the sky radiance and solar transmittance measured from ground, *J. Geophys. Res.*, 103, 31903–31923, 1998. 9842
- Dubovik, O., Smirnov, A., Holben, B. N., King, M. D., Kaufman, Y. J., Eck, T. F., and Slutsker, I.: Accuracy assessments of aerosol optical properties retrieved from Aerosol Robotic Net-
- 30

Retrieval of aerosol absorption properties

E. Rodríguez et al.

Title Page

Abstract

Introduction

Conclusions

References

Tables

Figures



Back

Close

Full Screen / Esc

Printer-friendly Version

Interactive Discussion



Retrieval of aerosol absorption properties

E. Rodríguez et al.

Title Page

Abstract

Introduction

Conclusions

References

Tables

Figures



Back

Close

Full Screen / Esc

Printer-friendly Version

Interactive Discussion



work (AERONET) Sun and sky radiance measurements, *J. Geophys. Res.*, 105, 9791–9806, 2000. 9842, 9847

Dubovik, O., Holben, B. N., Eck, T. F., Smirnov, A., Kaufman, Y. J., King, M. D., Tanre, D., and Slutsker, I.: Variability of absorption and optical properties of key aerosol types observed in worldwide locations, *J. Atmos. Sci.*, 59, 590–608, 2002. 9842

Dubovik, O., Sinyuk, A., Lapyonok, T., Sinyuk, A., Mishchenko, M. I., Yang, P., Eck, T. F., Volten, H., Munoz, O., Veihelmann, B., van der Zander, W. J., Sorokin, M., and Slutsker, I.: Application of light scattering by spheroids for accounting for particle non-sphericity in remote sensing of desert dust, *J. Geophys. Res.*, 111, D11208, doi:10.1029/2005JD006619, 2006. 9847

Goto, D., Takemura, T., Nakajima, T., and Badarinath, K. V. S.: Global aerosol model-derived black carbon concentration and single scattering albedo over Indian region and its comparison with ground observations, *Atmos. Environ.*, 45, 3277–3285, 2011. 9841

Jethva, H. and Torres, O.: Satellite-based evidence of wavelength-dependent aerosol absorption in biomass burning smoke inferred from Ozone Monitoring Instrument, *Atmos. Chem. Phys.*, 11, 10541–10551, doi:10.5194/acp-11-10541-2011, 2011. 9841

Holben, B., Eck, T., Slutsker, I., Tanre, D., Buis, J., Setzer, A., Vermote, E., Reagan, J., and Kaufman, Y.: AERONET a federated instrument network and data archive for aerosol characterization, *Remote. Sens. Environ.*, 66, 1–16, 1998. 9847

Holben, B., Tanre, D., Smirnov, A., Eck, T., Slutsker, I., Abuhassan, N., Newcomb, W., Schafer, J., Chatenet, B., Lavenue, F., Kaufman, Y., Vande Castle, J., Setzer, A., Markham, B., Clark, D., Frouin, R., Halthore, R., Karnieli, A., O'Neill, N., Pietras, C., Pinker, R., Voss, K., and Zibordi, G.: An emerging ground-based aerosol climatology: aerosol optical depth from AERONET, *J. Geophys. Res.*, 106, 12067–12097, 2001.

Huijnen, V., Flemming, J., Kaiser, J. W., Inness, A., Leitão, J., Heil, A., Eskes, H. J., Schultz, M. G., Benedetti, A., Hadji-Lazaro, J., Dufour, G., and Eremenko, M.: Hindcast experiments of tropospheric composition during the summer 2010 fires over western Russia, *Atmos. Chem. Phys.*, 12, 4341–4364, doi:10.5194/acp-12-4341-2012, 2012. 9847

IPCC: Climate Change 2007: The Physical Science Basis. Contribution of Working Group I to the Fourth Assessment Report of the Intergovernmental Panel on Climate Change, edited by: Solomon, S., Qin, D., Manning, M., Chen, Z., Marquis, M., Averyt, K. B., Tignor, M., and Miller, H. L., Cambridge University Press, Cambridge, UK and New York, NY, USA, 996 pp., 2007. 9840

Retrieval of aerosol absorption properties

E. Rodríguez et al.

Title Page

Abstract

Introduction

Conclusions

References

Tables

Figures



Back

Close

Full Screen / Esc

Printer-friendly Version

Interactive Discussion



- Kahn, R. A., Gaitley, B. J., Garay, M. J., Diner, D. J., Eck, T. F., Smirnov, A., and Holben, B. N.: Multiangle Imaging SpectroRadiometer global aerosol product assessment by comparison with the Aerosol Robotic Network, *J. Geophys. Res.*, 115, D23209, doi:10.1029/2010JD014601, 2010. 9841
- 5 Kolmonen, P., Sundström, A.-M., Sogacheva, L., Rodriguez, E., Virtanen, T., and de Leeuw, G.: Uncertainty characterization of AOD for the AATSR dual and single view retrieval algorithms, *Atmos. Meas. Tech. Discuss.*, 6, 4039–4075, doi:10.5194/amtd-6-4039-2013, 2013. 9842, 9843
- 10 Konovalov, I. B., Beekmann, M., Kuznetsova, I. N., Yurova, A., and Zvyagintsev, A. M.: Atmospheric impacts of the 2010 Russian wildfires: integrating modelling and measurements of an extreme air pollution episode in the Moscow region, *Atmos. Chem. Phys.*, 11, 10031–10056, doi:10.5194/acp-11-10031-2011, 2011. 9848
- 15 Krol, M., Peters, W., Hooghiemstra, P., George, M., Clerbaux, C., Hurtmans, D., McInerney, D., Sedano, F., Bergamaschi, P., El Hajj, M., Kaiser, J. W., Fisher, D., Yershov, V., and Muller, J.-P.: How much CO was emitted by the 2010 fires around Moscow?, *Atmos. Chem. Phys.*, 13, 4737–4747, doi:10.5194/acp-13-4737-2013, 2013. 9851
- Liu, Y., Huang, J., Shi, G., Takamura, T., Khatri, P., Bi, J., Shi, J., Wang, T., Wang, X., and Zhang, B.: Aerosol optical properties and radiative effect determined from sky-radiometer over Loess Plateau of Northwest China, *Atmos. Chem. Phys.*, 11, 11455–11463, doi:10.5194/acp-11-11455-2011, 2011. 9841
- 20 Matsueda, M.: Predictability of EuroRussian blocking in summer of 2010, *Geophys. Res. Lett.*, 38, L06801, doi:10.1029/2010GL046557, 2011.
- Medina, R., Fitzgerald, R. M., and Min, Q.: Retrieval of the single scattering albedo in the El Paso–Juarez Airshed using the TUV model and a UV-MFRSR radiometer, *Atmos. Environ.*, 25, 46, 430–440, 2012. 9841
- 25 Mei, L., Xue, Y., de Leeuw, G., Guang, J., Wang, Y., Li, Y., Xu, H., Yang, L., Hou, T., He, X., Wu, C., Dong, J., and Chen, Z.: Integration of remote sensing data and surface observations to estimate the impact of the Russian wildfires over Europe and Asia during August 2010, *Biogeosciences*, 8, 3771–3791, doi:10.5194/bg-8-3771-2011, 2011. 9847, 9848
- 30 Mielonen, T., Portin, H., Komppula, M., Leskinen, A., Tamminen, J., Jalongo, I., Hakkarainen, J., Lehtinen, K. E. J., and Arola, A.: Biomass burning aerosols observed in eastern Finland during the Russian wildfires in summer 2010 Part 2: Remote sensing, *Atmos. Environ.*, 47, 279–287, 2012. 9848

Retrieval of aerosol absorption properties

E. Rodríguez et al.

Title Page

Abstract

Introduction

Conclusions

References

Tables

Figures



Back

Close

Full Screen / Esc

Printer-friendly Version

Interactive Discussion



Patadia, F., Kahn, R. A., Limbacher, J. A., Burton, S. P., Ferrare, R. A., Hostetler, C. A., and Hair, J. W.: Aerosol airmass type mapping over the Urban Mexico City region from space-based multi-angle imaging, *Atmos. Chem. Phys.*, 13, 9525–9541, doi:10.5194/acp-13-9525-2013, 2013. 9841

Robles González, C.: Retrieval of Aerosol Properties Using ATSR-2 Observations and Their Interpretation, Ph. D. thesis, University of Utrecht, 2003. 9843

Russell, P. B., Bergstrom, R. W., Shinozuka, Y., Clarke, A. D., DeCarlo, P. F., Jimenez, J. L., Livingston, J. M., Redemann, J., Dubovik, O., and Strawa, A.: Absorption Angstrom Exponent in AERONET and related data as an indicator of aerosol composition, *Atmos. Chem. Phys.*, 10, 1155–1169, doi:10.5194/acp-10-1155-2010, 2010. 9841

Satheesh, S. K., Torres, O., Remer, L. A., Babu, S. S., Vinoj, V., Eck, T. F., Kleidman, R. G., and Holben, B. N.: Improved assessment of aerosol absorption using OMI-MODIS joint retrieval, *J. Geophys. Res.*, 114, D05209, doi:10.1029/2008JD011024, 2009. 9841

Torres, O., Decae, R., Veefkind, J. P., and de Leeuw, G.: OMI aerosolretrieval algorithm, in: OMI Algorithm Theoretical Basis Document: Clouds, Aerosols, and Surface UV Irradiance, Vol. 3, version 2, OMIATBD-03, edited by: Stammes, P., available at: http://eospsa.gsfc.nasa.gov/eos_homepage/for_scientists/atbd/docs/OMI/ATBD-OMI-03.pdf, NASA Goddard Space Flight Cent., Greenbelt, Md., 47–71, 2002a. 9846

Torres, O., Bhartia, P. K., Herman, J. R., Syniuk, A., Ginoux, P., and Holben, B.: A long term record of aerosol optical depth from TOMS observations and comparison to AERONET measurements, *J. Atmos. Sci.*, 59, 398–413, 2002b. 9846

Torres, O., Tanskanen, A., Veihelmann, B., Ahn, C., Braak, R., Bhartia, P. K., Veefkind, P., and Levelt, P.: Aerosols and surface UV products from ozone monitoring instrument observations: an overview, *J. Geophys. Res.*, 112, D24S47, doi:10.1029/2007JD008809, 2007. 9846

Torres, O., Ahn, C., and Chen, Z.: Improvements to the OMI near-UV aerosol algorithm using A-train CALIOP and AIRS observations, *Atmos. Meas. Tech.*, 6, 3257–3270, doi:10.5194/amt-6-3257-2013, 2013. 9841

Veefkind, J. P., de Leeuw, G. D., and Durkee, P. A.: Retrieval of aerosol optical depth over land using two-angle view satellite radiometry during TARFOX, *Geophys. Res. Lett.*, 25, 3135–3138, 1999. 9842, 9843

Veefkind, J. P., de Leeuw, G. D., Stammes, P., and Koelemeijer, R. B. A.: Regional distribution of aerosol over land, derived from ATSR-2 and GOME, *Remote Sens. Environ.*, 74, 377–386, 2000. 9843

Witte, J. C., Douglass, A. R., da Silva, A., Torres, O., Levy, R., and Duncan, B. N.: NASA A-Train and Terra observations of the 2010 Russian wildfires, *Atmos. Chem. Phys.*, 11, 9287–9301, doi:10.5194/acp-11-9287-2011, 2011. 9847, 9848

5 Zhu, L., Martins, J. V., and Remer, L. A.: Biomass burning aerosol absorption measurements with MODIS using the critical reflectance method, *J. Geophys. Res.*, 116, D07202, doi:10.1029/2010JD015187, 2011. 9841

10 Zvyagintsev, A. M., Blum, O. B., Glazkova, A. A., Kotel'nikov, S. N., Kuznetsova, I. N., Lapchenko, V. A., Lezina, E. A., Miller, E. A., Milyaev, V. A., Popikov, A. P., Semutnikova, E. G., Tarasova, O. A., and Shalygina, I. Yu.: Air pollution over european Russia and Ukraine under the hot summer conditions of 2010, *Izv. Atmos. Ocean. Phy.*, 47, 699–707, 2011. 9848

AMTD

7, 9839–9868, 2014

Retrieval of aerosol absorption properties

E. Rodríguez et al.

Title Page

Abstract

Introduction

Conclusions

References

Tables

Figures



Back

Close

Full Screen / Esc

Printer-friendly Version

Interactive Discussion



Retrieval of aerosol absorption properties

E. Rodríguez et al.

Title Page

Abstract

Introduction

Conclusions

References

Tables

Figures

I◀

▶I

◀

▶

Back

Close

Full Screen / Esc

Printer-friendly Version

Interactive Discussion



Table 1. Properties of the aerosol components used in this work (de Leeuw et al., 2014). Listed are the geometric radius r_g , standard deviation σ , refractive index n at the wavelength of $0.555 \mu\text{m}$, and the aerosol layer height (alh).

component	r_g (μm)	σ	n	alh (km)
weakly absorbing fine	0.07	1.700	1.40–0.003i	0–2
strongly absorbing fine	0.07	1.700	1.50–0.040i	0–2
sea salt	0.788	1.822	1.40–0.000i	0–2
dust	0.788	1.822	1.56–0.002i	2–4

Retrieval of aerosol absorption properties

E. Rodríguez et al.

Title Page

Abstract

Introduction

Conclusions

References

Tables

Figures



Back

Close

Full Screen / Esc

Printer-friendly Version

Interactive Discussion



Table 2. Wavelength dependence of the single scattering albedo SSA for the weakly and strongly absorbing fine mode aerosol components. The values are computed for the optical indices in Table 1.

wavelength	weakly absorbing	strongly absorbing
0.555 μm	0.977	0.796
0.659 μm	0.973	0.776
0.865 μm	0.966	0.738
1.610 μm	0.918	0.548

Retrieval of aerosol absorption properties

E. Rodríguez et al.

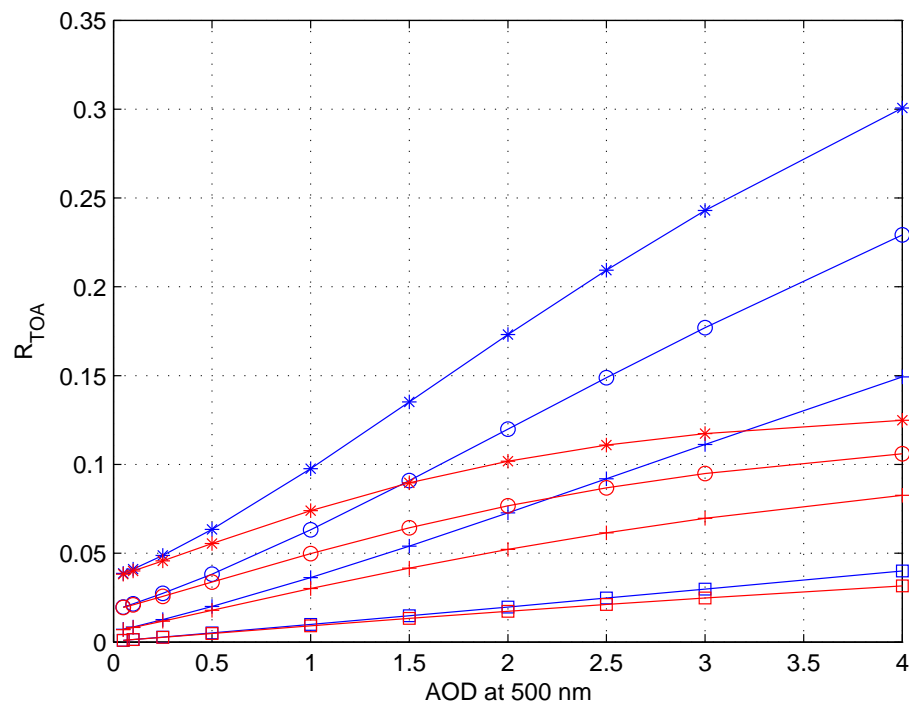


Figure 1. Calculated TOA reflectances for the weakly (blue) and strongly (red) absorbing fine mode aerosol components as function of the reference AOD at $0.500\ \mu\text{m}$ and for the four AATSR wavelengths: star $0.555\ \mu\text{m}$, circle $0.659\ \mu\text{m}$, plus $0.865\ \mu\text{m}$, and square $1.610\ \mu\text{m}$. In this example the geometry is set to a solar zenith angle of 30° , a satellite viewing zenith angle of 5° (near nadir), and a relative azimuth angle of 10° .

[Title Page](#)[Abstract](#)[Introduction](#)[Conclusions](#)[References](#)[Tables](#)[Figures](#)[◀](#)[▶](#)[◀](#)[▶](#)[Back](#)[Close](#)[Full Screen / Esc](#)[Printer-friendly Version](#)[Interactive Discussion](#)

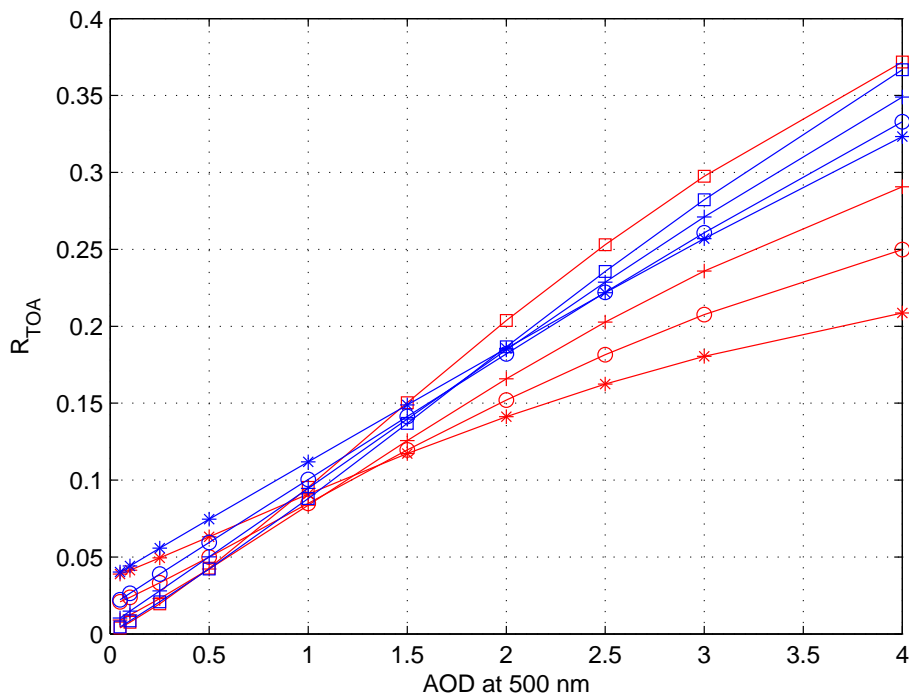


Figure 2. Modeled top-of-atmosphere (TOA) reflectances for the sea salt (blue) and dust (red) coarse aerosol components as function of the reference AOD at $0.500\ \mu\text{m}$. The wavelength dependency of reflectance is indicated by symbols: star $0.555\ \mu\text{m}$, circle $0.659\ \mu\text{m}$, plus $0.865\ \mu\text{m}$, and square $1.610\ \mu\text{m}$. In this example the geometry is set to a solar zenith angle of 30° , a satellite viewing zenith angle of 5° (near nadir), and a relative azimuth angle of 10° .

Retrieval of aerosol absorption properties

E. Rodríguez et al.

Title Page	
Abstract	Introduction
Conclusions	References
Tables	Figures
◀	▶
◀	▶
Back	Close
Full Screen / Esc	
Printer-friendly Version	
Interactive Discussion	



Retrieval of aerosol absorption properties

E. Rodríguez et al.

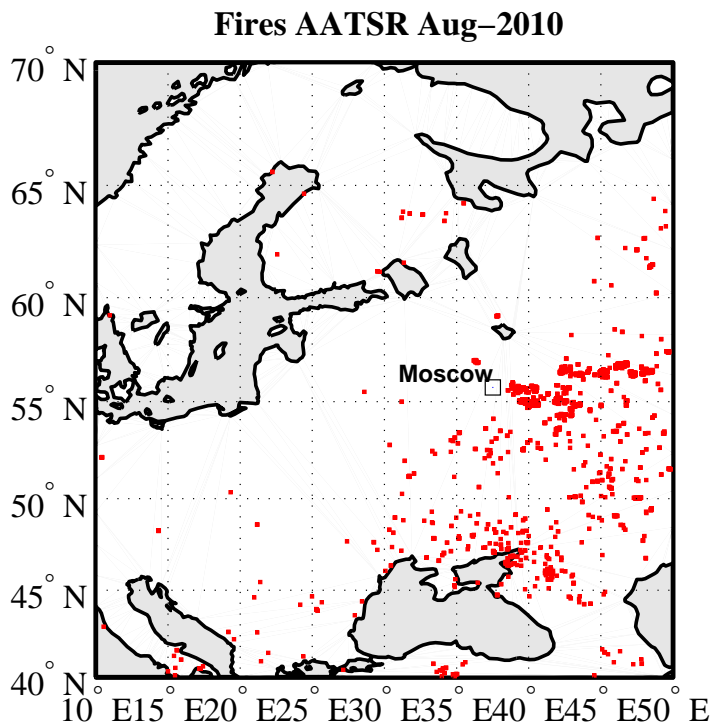


Figure 3. The occurrence of forest fires over western Russia during August 2010. Source: AATSR world fires Atlas (AATSR-WFA).

[Title Page](#)[Abstract](#)[Introduction](#)[Conclusions](#)[References](#)[Tables](#)[Figures](#)[◀](#)[▶](#)[◀](#)[▶](#)[Back](#)[Close](#)[Full Screen / Esc](#)[Printer-friendly Version](#)[Interactive Discussion](#)

Retrieval of aerosol absorption properties

E. Rodríguez et al.

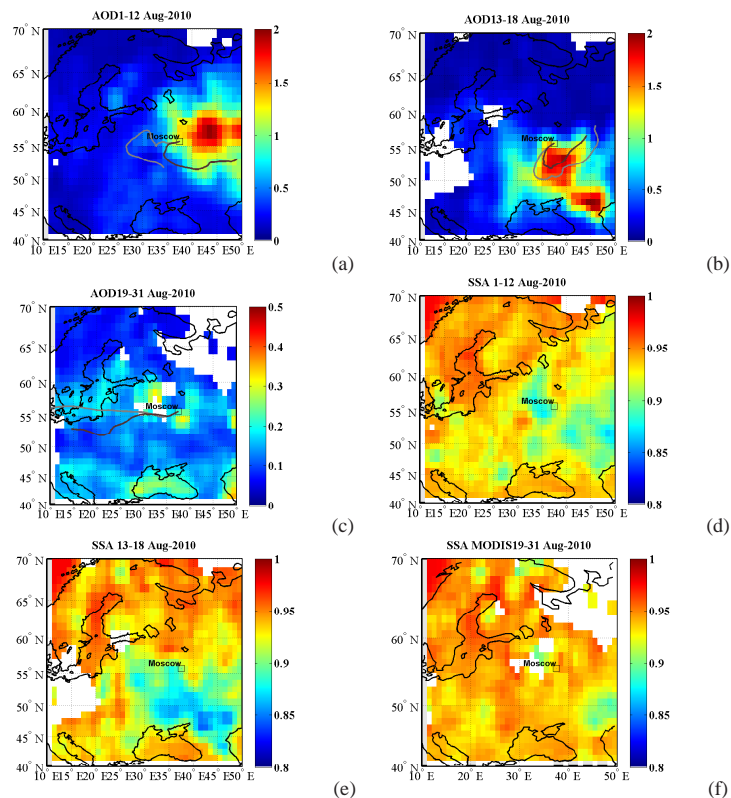
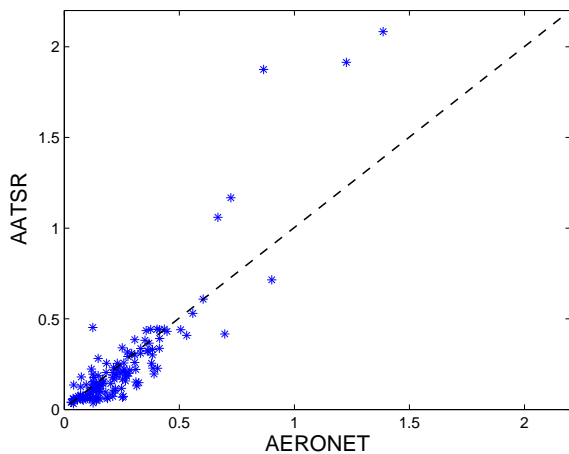
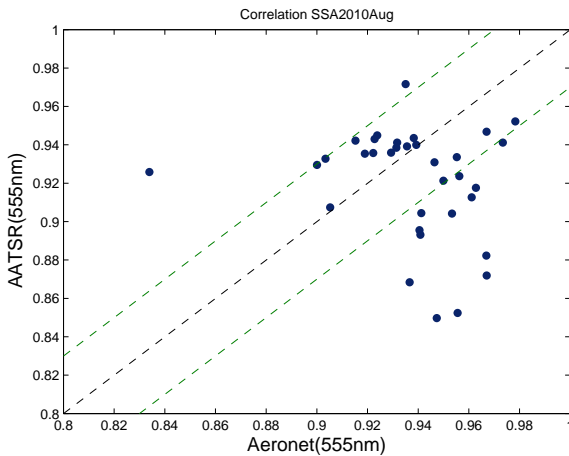


Figure 4. Spatial distributions of AOD and SSA at $0.555\ \mu\text{m}$ over the wildfires region, shown as aggregates for three periods in August 2010. Figure (a–c) presents the AOD during the wildfires (a, b) and after the fires extinguished (c). 5 day back-trajectories at 500 m (in purple) and 100 m (in grey) are overlaid on the AOD maps. Figure (d–f) presents the SSA for the same periods.



a



b

Figure 5. Comparison of AOD and SSA at 555 nm retrieved from AATSR and AERONET.

Retrieval of aerosol absorption properties

E. Rodríguez et al.

Title Page

Abstract

Introduction

Conclusions

References

Tables

Figures



Back

Close

Full Screen / Esc

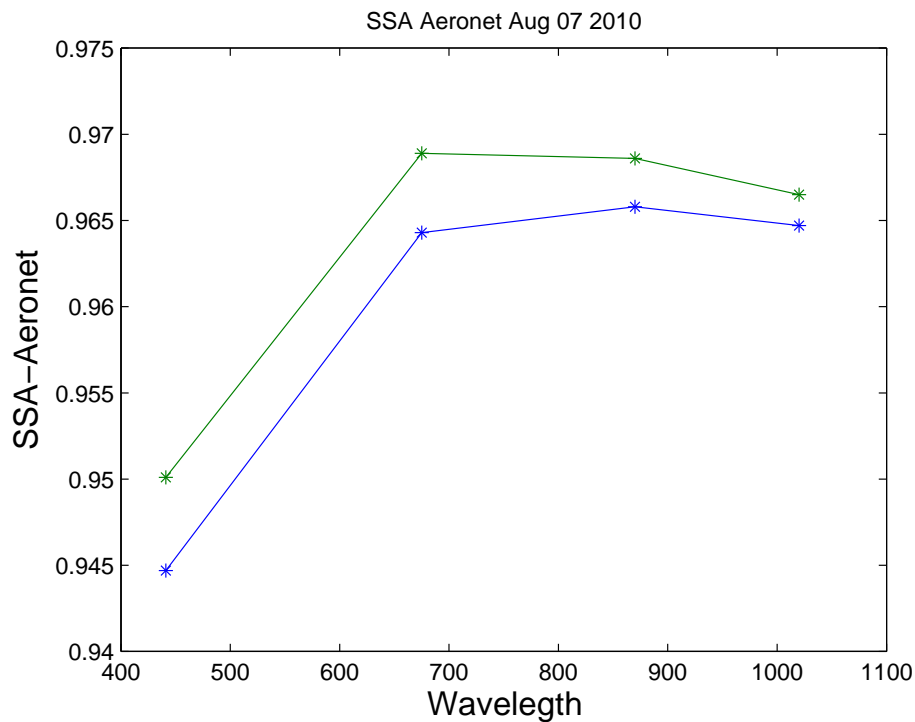
Printer-friendly Version

Interactive Discussion



Retrieval of aerosol absorption properties

E. Rodríguez et al.

**Figure 6.** SSA wavelength dependence of the AERONET inversion product for 7 August 2010.[Title Page](#)[Abstract](#)[Introduction](#)[Conclusions](#)[References](#)[Tables](#)[Figures](#)[Back](#)[Close](#)[Full Screen / Esc](#)[Printer-friendly Version](#)[Interactive Discussion](#)

Retrieval of aerosol absorption properties

E. Rodríguez et al.

Title Page

Abstract

Introduction

Conclusions

References

Tables

Figures

◀

▶

◀

▶

Back

Close

Full Screen / Esc

Printer-friendly Version

Interactive Discussion

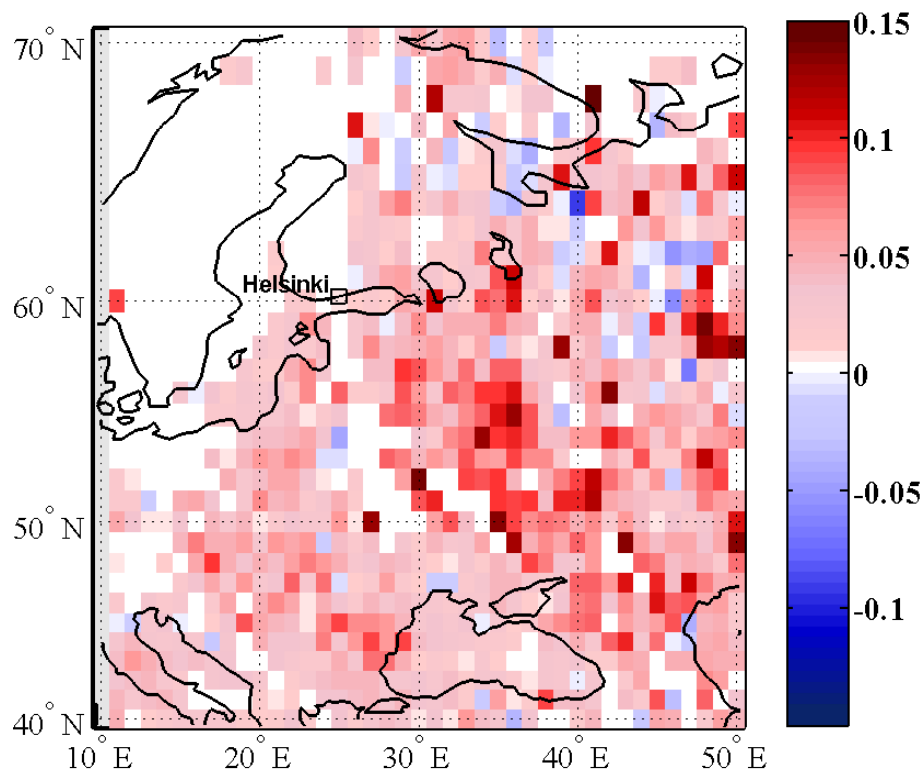


Figure 7. SSA difference between the SSA retrieved with OMI and AATSR in August 2010 (OMI-AATSR). Large differences between the retrievals occur in the areas where absorbing aerosol particles are expected due to the occurrence of forest fires.

Retrieval of aerosol
absorption properties

E. Rodríguez et al.

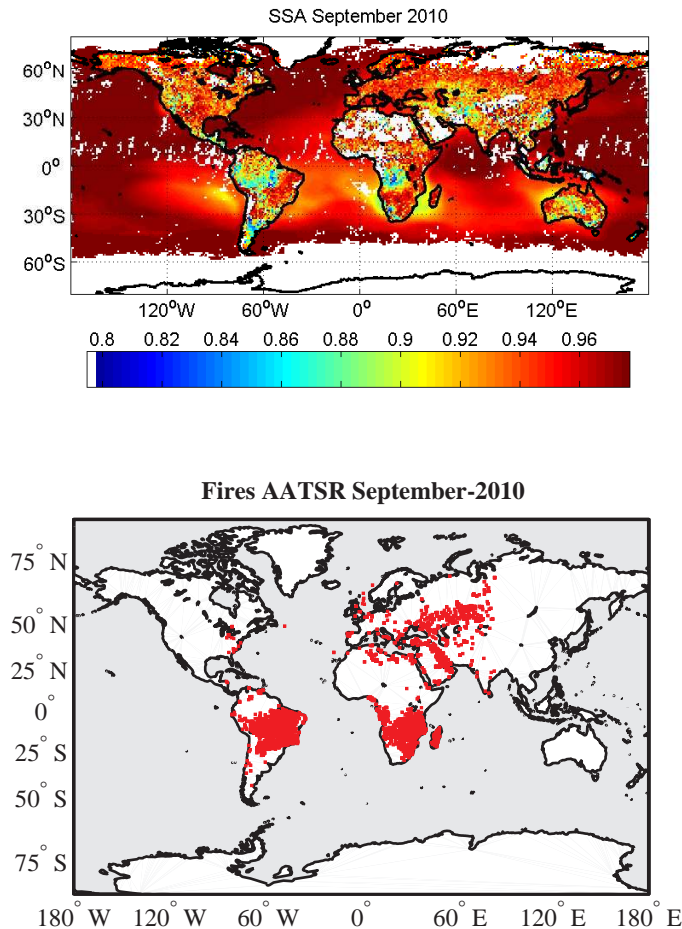


Figure 8. (Top) Global SSA retrieved for September 2010. (bottom) Global forest fires map for September 2010 using AATSR-WFA.

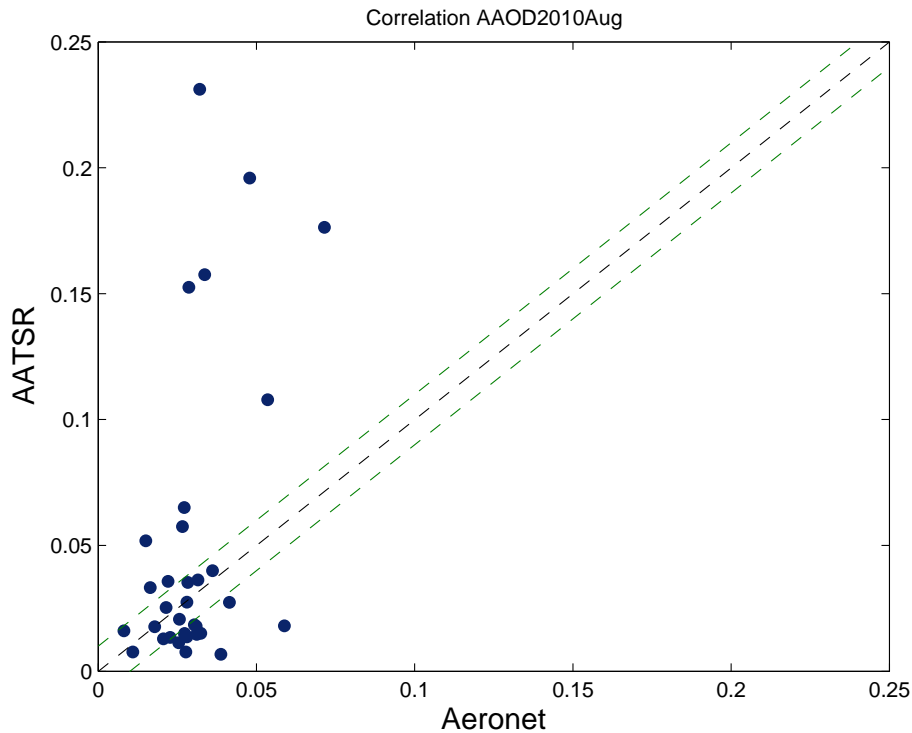


Figure 9. Comparison of AAOD retrievals from AATSR and AERONET over Moscow in August 2010.

Retrieval of aerosol absorption properties

E. Rodríguez et al.

Title Page	
Abstract	Introduction
Conclusions	References
Tables	Figures
◀	▶
◀	▶
Back	Close
Full Screen / Esc	
Printer-friendly Version	
Interactive Discussion	

